Thermodynamic Basis for Sequence-Specific Recognition of ssDNA by an Autoantibody†

P. Christine Ackroyd,‡,§ Joanne Cleary,‡,§ and Gary D. Glick*,‡,||

Departments of Chemistry and Biological Chemistry, The University of Michigan, 930 North University Avenue, Ann Arbor, Michigan 48109-1055

Received October 13, 2000; Revised Manuscript Received January 17, 2001

ABSTRACT: 11F8 is a sequence-specific DNA binding monoclonal autoantibody previously isolated from an autoimmune lupus-prone mouse [Stevens, S. Y., and Glick, G. D. (1999) *Biochemistry 38,* 560−568]. This antibody, like many other lupus anti-DNAs, localizes to kidney tissue and eventually leads to renal damage through a process that first involves the binding of DNA antigens. A series of experiments were conducted to investigate the thermodynamic and structural basis by which this antibody discriminates between specific, noncognate, and nonspecific sequences. Sequence-specific binding occurs with a minimal dependence on the polyelectrolyte effect along with a favorable binding enthalpy reflecting the presence of base stacking and contacts to DNA bases. This favorable binding enthalpy apparently is derived from desolvation at the binding interface and is consistent with recent models of the nonclassical hydrophobic effect. Noncognate recognition is also driven by the nonclassical hydrophobic effect, but is accompanied by highly unfavorable entropies that are responsible for reduced affinity relative to the high-affinity consensus sequence. Nonspecific recognition is driven completely by the polyelectrolyte effect involving extensive electrostatic interactions with the phosphate backbone. Collectively, the data demonstrate the ability of 11F8 to adapt its mode of binding to the available DNA surface and provide a thermodynamic model for sequence-specific recognition of single-stranded DNA. The salient features of this model employ the paradigms invoked to explain protein·dsDNA, protein·RNA, and antibody·antigen binding.

Understanding the structural and thermodynamic basis of protein·nucleic acid recognition is of fundamental importance to cellular regulation. Thermodynamic and structural measurements have been conducted on a variety of nucleic acid recognition systems to elucidate the factors that both regulate binding affinity and allow nucleic acid binding proteins to distinguish between target and competing sequences (specificity). Double-stranded DNA (dsDNA)[1] binding proteins use a balance of forces to achieve high affinity and specificity. Sequence-specific recognition of dsDNA is generally entropically driven due to the polyelectrolyte and hydrophobic effects, which promote maximum surface complementarity at the protein·DNA interface (*1*−*3*). However, several examples of enthalpically driven sequence-specific dsDNA recognition have been reported (*4*−*6*). In general, recognition of dsDNA is dominated by 'direct readout' of the sequence, a process that involves matching complementary arrays of hydrogen bonds between a given protein and a dsDNA sequence (*7*, *8*). In contrast, nonspecific recognition of the phosphate backbone is largely driven by the polyelectrolyte effect (*7*−*11*).

Protein·RNA recognition differs from dsDNA recognition because RNA can fold into complex secondary structures. Both single-stranded and double-stranded RNA regions are recognized by proteins, and structural features such as three-dimensional shape and charge distribution provide critical features for sequence discrimination (*12*). Binding energy is often provided by hydrogen bonding, a relatively small dependence on the polyelectrolyte effect, and the interaction of protein side chains with RNA bases (*12*, *13*). Conformational reorganization to achieve maximum complementary is common for both protein and RNA binding partners (*14*). Consequently, a key determinant of specificity can be the energetic costs paid to achieve an appropriate bound conformation (*15*).

Sources of sequence specificity for single-stranded DNA (ssDNA) binding proteins are less well understood. The majority of highly characterized ssDNA binding proteins, such as *E. coli* SSB, gene32 protein, and geneV protein, bind cooperatively to ssDNA (*16*−*19*). Binding energy is contributed by cation release from the phosphate backbone and stacking of aromatic side chains with DNA bases (*20*−*23*). Although these proteins often display discrimination for one homopolymer over another, no sequence specificity exists (*9*). A large number of proteins that interact sequence-specifically with ssDNA have been reported (e.g., *24*−*28*). However, a systematic evaluation of the thermodynamic and structural basis for sequence-specific recognition has yet to be described.

† Supported by NIH Grant GM 42168.

* Address correspondence to this author. Phone: (734)764-4548; Fax: (734)763-2307; E-mail: gglick@umich.edu.

‡ Department of Chemistry.

§ Both authors made significant contributions to this work.

|| Department of Biological Chemistry.

[1] Abbreviations: anti-DNA, anti-DNA autoantibodies; DEPC, diethyl pyrocarbonate; DMS, dimethyl sulfate; dsDNA, double-stranded DNA; ssDNA, single-stranded DNA; mAbs, monoclonal antibodies; CDR, complementarity determining region; $KMnO_4$, potassium permanganate; SLE, systemic lupus erythematosus.

10.1021/bi0023854 CCC: $20.00 © 2001 American Chemical Society
Published on Web 02/10/2001

Antibodies that bind DNA (anti-DNA) provide a unique framework to characterize protein·nucleic acid interactions. Anti-dsDNA and anti-ssDNA are spontaneously produced by patients with the autoimmune disorder systemic lupus erythematosus (SLE), and in some instances, these autoantibodies can be pathogenic (*29*). In particular, a subset of anti-DNA localize to kidney tissue through a process involving binding to DNA or DNA-containing antigens (*30*−*32*). Hence, defining the molecular basis of DNA recognition by lupus autoantibodies could provide insight into the pathogenic nature of anti-DNA antibodies as well as recognition of DNA in general. However, little is known about the thermodynamic, kinetic, or structural basis of DNA recognition by lupus autoantibodies. Using binding site selection experiments, we have previously investigated the sequence specificity of three clonally related monoclonal anti-ssDNA antibodies (*33*). One of these antibodies, 11F8, binds sequence-specifically to a ssDNA motif, designated **WT** (Figure 1). NMR and chemical footprinting experiments indicate that **WT** forms a stem−loop structure (*33*). Here we describe experiments to elucidate the thermodynamic basis by which 11F8 discriminates between the specific sequence (**WT**) and alternative sequences. Collectively, these data provide a thermodynamic model for sequence-specific recognition of single-stranded DNA, the salient features of which employ the paradigms used to describe protein·dsDNA, protein·RNA, and antibody·antigen binding.

MATERIALS AND METHODS

11F8 and DNA Preparation. 11F8 was isolated from ascites fluid and purified by affinity chromatography (>95%) as previously described (*34*). 11F8 concentrations were calculated from the absorbance at 280 nm, with an extinction coefficient (0.67 mg·mL^{-1}/OD$_{280}$) that was calculated from the amino acid sequence (*35*). Concentrations calculated from the absorbance were identical to those measured using Bradford assays (Bio-Rad, Hercules, CA). The DNA sequences were synthesized using standard protocols and purified to >95% by HPLC, as previously described (*33*). To ensure that the DNA counterion was sodium, purified DNA was equilibrated in 4 M NaCl overnight and desalted by gel filtration with Sephadex Superfine 450 (Pharmacia, Piscataway, NJ) or NAP-5 columns (Amersham Pharmacia, Upsalla, Sweden). DNA concentrations were calculated from the DNA absorbance at 260 nm, using extinction coefficients calculated from the DNA sequence (*36*). DNA solutions were heated to 95 °C prior to measurement to avoid the effects of DNA secondary structure on absorbance.

Steady-State Fluorescence Affinity Measurement. Fluorescence measurements were carried out on a Spectronic AB2 fluorometer equipped with a magnetic stirrer and thermostated cell block. Briefly, 11F8 was diluted into titration buffer (20 mM Tris, variable [MX] and pH) and allowed to equilibrate at the experimental temperature. The intrinsic protein fluorescence (λ_{em} 338 nm; 16 nm band-pass) was measured as a function of added DNA. Excitation wavelengths were chosen such that the absorption of excitation light by DNA was not prohibitive. In general, **WT** titrations used 280 or 295 nm excitation, **LS** and **T7** used 295 or 305 nm excitation, while **NS** and weakly binding DNA mutants used 305 or 310 nm excitation. Control experiments showed no dependence of the observed K_d on the choice of excitation wavelength. Final fluorescence values were calculated according to eq 1:

$$F_{corr} = (F_{uncorr} - F_{bkgd})\cdot(\text{IF corr})\cdot(V_i/V_{init}) \quad (1)$$

where F_{bkgd} = fluorescence of DNA titrated into buffer, V_i = reaction volume at each point, V_{init} = initial reaction volume, and IF corr = inner filter correction = $1/(1 - 10^{-A})$ (*37*) where A = solution absorbance at the excitation wavelength.

Dissociation constants were obtained from fluorescence intensity values with an iterative protocol using eqs 2−5 as previously described (*38*). Quenching values (eq 2) were first plotted vs the values of free DNA concentration calculated using eqs 3 and 4 and an initial estimate for Q_{max}. A fit of the single-site binding isotherm (eq 5) to these data by nonlinear least-squares regression using the computer program Kalaidagraph yielded a more accurate value of Q_{max}. This new value of $Q_{max}$was used to calculate final free DNA concentration values, and an additional fit of the single-site binding isotherm to quenching and free DNA concentration values yielded the dissociation constant:

$$Q_i = (F_{init} - F_i)/F_{init} \quad (2)$$

$$Q_i/Q_{max} = \text{fraction bound} = [\text{bound mAb}]/[\text{total protein sites}] \quad (3)$$

$$[\text{free DNA}] = [\text{total DNA}] - Q_i/Q_{max}[\text{mAb}]_{total} \quad (4)$$

$$Q_I = Q_{max}[\text{free DNA}]/(K_d + [\text{free DNA}]) \quad (5)$$

where Q_i = fluorescence quenching at each added DNA concentration, F_{init} = protein fluorescence in the absence of added DNA, F_i = fluorescence at each added DNA concentration, and [total protein sites] was kept below the K_d and was equal to twice the [mAb]$_{total}$. Error bars reported for dissociation constants are the standard error based on a minimum of three replicates.

van't Hoff Experiments. Titrations were carried out from 5 to 35 °C (20 mM Tris; pH and [NaCl] varying with system). To correct for pH variation of the buffer with temperature, separate buffers were made at each titration temperature. Data were plotted in van't Hoff form (ln K_{obs} vs 1/T) and analyzed using the computer program Kalaidagraph. Enthalpy values were obtained from the data using either the van't Hoff equation (eq 6), or a series of relationships that assumes constant heat capacity change (eqs 7 and 8) (*3*):

$$(\delta \ln K_{obs}/\delta\, 1/T)_P = -\Delta H^\circ_{obs}/R \quad (6)$$

$$\ln K_{obs} = \Delta C^\circ_p/R[T_H/T - \ln(T_S/T) - 1] \quad (7)$$

$$\Delta H^\circ_{obs} = \Delta C^\circ_p(T - T_H) \quad (8)$$

$$\Delta G^\circ_{obs} = \Delta H^\circ_{obs} - T\Delta S^\circ_{obs} \quad (9)$$

where T_H is the temperature at which the enthalpic driving force is zero and T_S is the temperature at which the entropic

driving force is zero (*39*); T_H and T_S are obtained from a fit of the data to eq 7. Entropy values were obtained from free energy and enthalpy values according to eq 9. Errors reported for $\Delta H°_{obs}$, $\Delta C°_p$, T_H, and T_S reflect either uncertainty associated with nonlinear least-squares regression to eq 7, or the standard deviation of the slope of the linear van't Hoff plot. Errors for $\Delta G°_{obs}$ are 95% confidence limits calculated from a minimum of three K_d measurements. Reported errors in $T\Delta S°_{obs}$ are propagated from errors associated with $\Delta H°_{obs}$ and $\Delta G°_{obs}$.

Osmotic Pressure and Polarity Experiments. Affinity was determined by fluorescence titration, using titration buffer that contained varying amounts of glycerol, methanol, ethanol, or 1-propanol. Osmolal concentrations were calculated from the solvent weight percent using published tables (*40*). Values for the dielectric constant(s) of aqueous solvent mixtures were calculated from empirical relationships based on weight percent (*41*). Since experiments with different solvents were carried out at identical buffer salt concentrations, the contribution of buffer salt concentration to the bulk dielectric constant was neglected. Errors reported for these data are the standard deviations of the slope obtained by linear regression of a minimum of four points.

UV Thermal Denaturation Studies. Melting studies were conducted using a Carey 3 spectrophotometer. DNA samples were diluted in filtered buffer (20 mM Tris, 150 mM NaCl, pH 8) in sealed semi-micro cuvettes and mixed by inversion. DNA concentrations were sufficient to have final A_{260} values ranging from 0.2 to 0.5 OD. Solutions were equilibrated at 5 °C for 30 min, and A_{260} was measured as the temperature was ramped from 5 to 95 °C (1 °C/min). The absorbance signal was measured twice per minute with 3 s average time (4 nm bandwidth). After data collection, T_m values were calculated from the first derivative of the melting curve using the spectrophotometer software.

CD Studies. CD spectra of 11F8, DNA, and 1:1 11F8·DNA complexes (5 μM) were measured in titration buffer (20 mM Tris, 150 mM NaCl, pH 8, 5 °C) on an AVIV 62DS spectrometer. Individual spectra were the average of three scans, with data collected every nanometer (3 s averaging time). Spectra of 11F8·DNA complexes and the sum of 11F8 and DNA spectra were compared after correction for buffer signal and differences in dynode voltage.

Footprinting DNA Ligands and mAb·DNA Complexes. 11F8 and 5′ ^{32}P end-labeled DNA were incubated in buffer (10 mM Tris, pH 8; 150 mM NaCl) containing dA_{21} as a nonspecific competitor (1 μM). In these experiments, excess protein was used to ensure that all DNA was bound. Potassium permanganate footprinting was then performed as previously described (*42*), either in the absence or in the presence of protein. The chemically modified DNA isolated from the footprinting reaction was electrophoresed on a denaturing gel [15% 19:1 acrylamide/bis(acrylamide), 8 M urea−polyacrylamide gel in 1 × TBE] at a constant power of 63 W for 2 h. The gels were analyzed using a Molecular Dynamics phosphorimager as previously described (*42*, *43*).

RESULTS

Selection of DNA Sequences. Experiments were conducted comparing the binding of **WT** and a group of different DNA constructs (Figure 1). A nonspecific ligand, 5′(GATC)$_{13}$GAT

FIGURE 1: DNA sequences used in binding studies. **WT** is the 55 base-long construct obtained from binding site selection experiments with 11F8 (*33*). Additional nucleotides flanking the selected stem−loop are not shown (represented as ~) and are part of the PCR primers used in original binding site selection experiments. **T7** replaces positions 3, 8−14, and 16 of **WT** with T, resulting in a T-rich linear sequence. In **LS**, positions 3 and 16 of **WT** are replaced with T to preclude secondary structure formation.

(designated **NS**), represents all bases equally and does not possess any secondary structure. Additional ligands are variants of **WT** and can be considered 'noncognate' sites since they differ from **WT** at only a few positions and are bound by 11F8 with slightly lower affinity than **WT**. **LS** contains base-pair mismatches in the stem duplex of **WT** and does not adopt a stem−loop secondary structure. This sequence was designed to probe the energetics of preorganizing the binding epitope within **WT** into a defined secondary structure. A second variant of **WT**, designated **T7**, replaces nucleotides 8−14 with thymine. In addition, nucleotides 3 and 16 were also replaced with thymine to prevent stem duplex formation. Previous studies have established that 11F8, similar to other ssDNA binding proteins, displays a base preference for thymine (*34*). Discrimination between a "preferred" homopolymer and a specific sequence has been proposed to represent another aspect of specificity relative to random sequence DNA (*33*). Therefore, **T7** was chosen to examine recognition of this preferred homopolymer, within a context similar to **WT**. In addition to these constructs, various loop, stem, and bulge mutants were constructed to help identify individual nucleotides that may contact 11F8 directly as well as those that contribute to recognition through **WT** secondary structure. In particular, mutants T11dU and ΔdG_4, which lacks the **WT** bulge, were studied, since both the T11 methyl group and bulge are necessary for high-affinity **WT** binding (vide infra).

Quenching of the intrinsic protein fluorescence was used to measure 11F8 binding affinity (*34*). This method does not require physical separation of bound and free ligand, allowing affinity constants to be measured at equilibrium. Representative binding isotherms for 11F8 binding to **WT**, **NS**, **LS**, and **T7** are shown in Figure 2 and K_d values are listed in Table 1. The (thermodynamic) measure of specificity represents the degree to which a protein can discriminate between a 'specific' site, those of similar composition, and random DNA (*1*, *2*). The ratio between specific and nonspecific binding affinities ranges from 3 (*44*) to $\geq 10^2$ (*1*, *2*, *12*, *45*, *46*) for nucleic acid binding proteins. The specificity ratios for 11F8 binding to **WT** compared to **NS** and **T7** are 600 and 4, respectively. 11F8 binding to **LS** occurs with 10-fold lower affinity than **WT**, which suggests

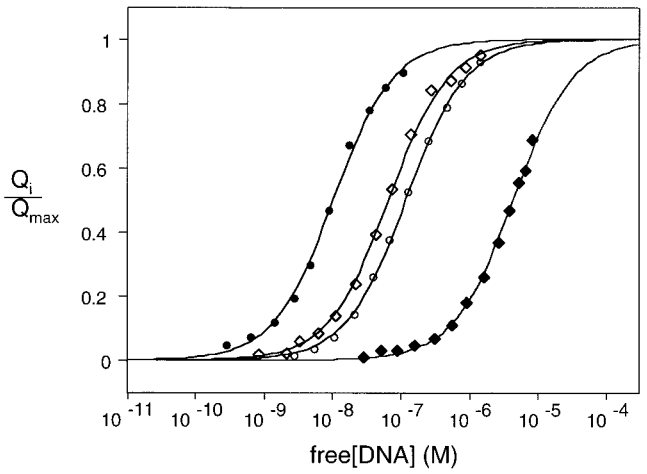

FIGURE 2: Representative 11F8 binding isotherms for **WT** (●), **T7** (◇), **LS** (○), and **NS** (◆). Data were measured in standard titration buffer (20 mM Tris, 150 mM NaCl, 25 °C, pH 8). Since 11F8 occludes about five nucleotides upon binding (*34*), overlapping binding sites are possible for **T7** and **NS**. Therefore, fit of the single-site binding isotherm yields apparent K_d values that overestimate single site affinity for these sequences. High DNA absorbance at 305 nm prevented measurement of additional points on the **NS** titration curve.

Table 1: Relative Affinities and Salt Release Stoichiometries for 11F8 Complexes[a]

DNA	salt	$-SK_{obs}$	K_d (nM)	relative K_d
WT	NaCl	2.18 ± 0.07	10.1 ± 0.6	1
	NaOAc	1.4 ± 0.1		
LS	NaCl	2.29 ± 0.06	119 ± 5	12
	NaOAc	2.1 ± 0.2		
T7	NaCl	3.4 ± 0.1	46 ± 5	4.6
	NaOAc	2.9 ± 0.2		
ΔdG_4	NaCl	2.6 ± 0.1	90 ± 10	9
	NaOAc	2.2 ± 0.2		
T11dU	NaCl	2.4 ± 0.2	71 ± 25	7
	NaOAc	2.2 ± 0.1		
NS	NaCl	7.3 ± 0.1	6300 ± 700	570
	NaOAc	7.0 ± 0.2		

[a] Affinity measurements were carried out in Tris buffer (20 mM Tris, 85−400 mM [MX], pH 8 or 8.3, 25 °C). Values of $-SK_{obs}$ represent the stoichiometry of salt release as described by Record (*52*) and were obtained from the slope of plots shown in Figure 3. Values of K_d were obtained in 20 mM Tris, 150 mM NaCl, pH 8 at 25 °C. Relative K_d values are normalized against **WT**. Errors in K_d are the standard error based on a minimum of three trials. Errors in $-SK_{obs}$ are the standard deviations associated with slope of the salt plots. No evidence for changes in 11F8 conformation with salt concentration was detected by CD.

that preorganization of the recognition site is important for high-affinity binding (Table 1). Together, these data indicate that specific DNA binding by 11F8 is achieved only when the appropriate recognition elements on **WT** are presented within a defined secondary structure.

11F8 Binding as a Function of Temperature. To determine the enthalpic and entropic driving force for 11F8 recognition of DNA, affinity measurements were conducted as a function of temperature. A comparison of the van't Hoff data for **WT**, **T7**, **LS**, **NS**, T11dU, and ΔdG_4 demonstrates distinct differences in thermodynamic behavior (Figure 3). The van't Hoff plot (ln K_{obs} vs $1/T$) for the 11F8·**WT** complex shows both a positive slope and a deviation from linearity, reflecting a favorable enthalpic driving force and a negative change in heat capacity (Figure 3a). Recognition of **LS** is accompanied by similar temperature dependence; however, the maximum in the **LS** van't Hoff plot occurs at a lower temperature than the corresponding maximum for **WT**. The van't Hoff plots for **T7**, T11dU, and ΔdG_4 are linear, with a positive slope that reflects a favorable enthalpy change accompanying binding (Figure 3b,c). These data suggest that for these sequences, no net heat capacity change is associated with complexation. Recognition of **NS** is not temperature dependent from 10 to 30 °C (Figure 3b), which indicates that $\Delta H \cong 0$ and recognition of this sequence is entropy-driven.

The temperature data for **WT** and **LS** were fit to a model that assumes a constant heat capacity change, and the resulting enthalpy, heat capacity, and entropy values are shown in Table 3. Binding of **WT** is enthalpically favorable and opposed by entropy. It was anticipated that the entropic cost for binding **LS** would be higher than for binding **WT**. As expected, the entropy associated with 11F8·**LS** binding is more unfavorable than for 11F8·**WT**. However, ΔH is more favorable for **LS** than for **WT**, which partly compensates for the higher entropic cost associated with recognition of this unstructured sequence. Hence, the interaction of 11F8 with **WT** may represent a compromise between maximizing favorable interactions at the binding interface and the entropic cost associated with recognition of ssDNA.

Apparent linearity of the van't Hoff plot, as shown for **T7**, ΔdG_4, and T11dU, may result from zero heat capacity or from experimental temperatures that are well above the plot maximum (T_H). A zero heat capacity change accompanying binding of **T7**, ΔdG_4, and T11dU is supported by the observation that data analysis using eq 7, which allows for the possibility of a heat capacity change, produces $\Delta C°_p$ values that are indistinguishable from zero (data not shown). Regardless, the assumption of linearity will produce appropriate values for the enthalpy and entropy changes, because the enthalpy change at any temperature is proportional to the instantaneous slope (eq 6). Hence, the temperature data for **T7**, ΔdG_4, and T11dU were fit to a model that assumes a zero $\Delta C°_p$. As observed for **WT** and **LS**, 11F8 recognition of these noncognate sequences is driven by enthalpy and opposed by entropy (Table 2). Favorable enthalpies have been observed for noncognate DNA binding of other proteins, including several nonspecific ssDNA helicases (*47*, *48*), dsDNA transcription factors (*4*, *5*), and an engineered anti-ssDNA antibody (*49*).

A variety of possible effects may contribute to the thermodynamic parameters associated with 11F8 binding. These processes include hydrogen bonding, van der Waals interactions, intercalation of DNA nucleotides between aromatic amino acids within the 11F8 binding site (i.e., base-stacking) (*50*, *51*), losses in rotational, translational, and vibrational degrees of freedom, and release or uptake of water molecules and ions (*3*, *9*). A series of experiments varying both solution conditions and DNA sequence were conducted to elucidate the components that comprise the observed enthalpy and entropy changes.

11F8 Binding as a Function of Salt Concentration. Cations condensed along the DNA backbone that are released into bulk solution upon binding can provide a large entropic driving force for protein·DNA complexation. The sensitivity of binding affinity to buffer salt concentration reflects the involvement of the polyelectrolyte effect, where the slope of the plot $-\ln K_{obs}$ versus ln [MX] represents the stoichi-

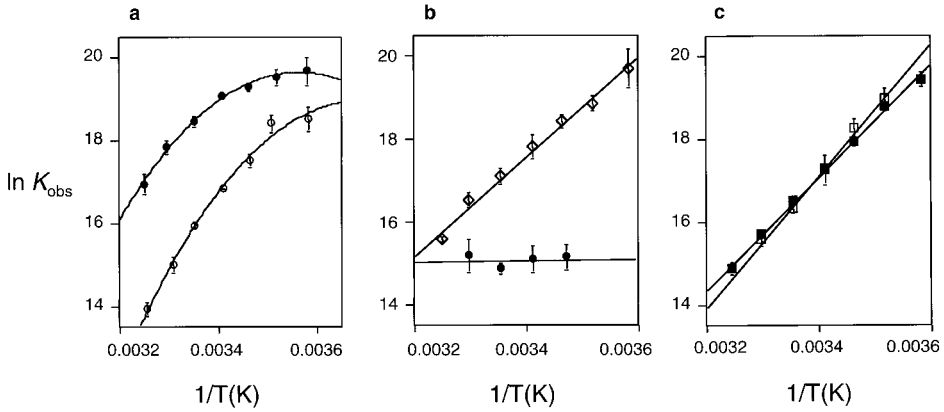

FIGURE 3: van't Hoff analysis of 11F8 binding. (a) Data for **WT** (●) and **LS** (○) were measured in 20 mM Tris, 150 mM NaCl, pH 8, and analyzed assuming a constant negative heat capacity. (b) Data for **T7** (◇) were measured in 20 mM Tris, 150 mM NaCl, pH 8, and analyzed assuming no heat capacity change. Data for **NS** (◆) were measured in 20 mM Tris, 100 mM NaCl, pH 8. (c) Data for ΔdG_4 (■) and T11dU (□) were measured in 20 mM Tris, 150 mM NaCl at pH 8 and analyzed assuming no heat capacity change. Error bars shown represent 95% confidence limits based on a minimum of three trials.

Table 2: Thermodynamic Parameters Associated with 11F8 Binding at 25 °C[a]

sequence	$\Delta G°_{obs}$ (kcal/mol)	$\Delta H°_{obs}$ (kcal/mol)	$T\Delta S°_{obs}$ (kcal/mol)	$\Delta C_p°$ [kcal/(mol·K)]	T_H (°C)	T_S (°C)
WT	-10.91 ± 0.02	-22 ± 2	-11 ± 2	-1.3 ± 0.1	8 ± 1	16.5 ± 0.5
LS	-9.45 ± 0.02	-36 ± 9	-27 ± 9	-1.3 ± 0.3	-3 ± 1	5.3 ± 0.9
T7	-10.00 ± 0.08	-23 ± 3	-13 ± 3	0	–	–
ΔdG_4	-9.64 ± 0.05	-27.0 ± 0.3	-17.4 ± 0.3	0	–	–
T11dU	-9.67 ± 0.01	-31.7 ± 0.5	-22 ± 0.5	0	–	–
NS	-7.09 ± 0.05	0	7 ± 1	0	–	–

[a] Errors for ΔG are the standard deviations normalized for the number of trials (standard error). Enthalpy data were obtained by van't Hoff analysis over the temperature range 5−35 °C as shown in Figure 5. Errors reported for ΔH, ΔC_p, T_H, and T_S reflect either uncertainty associated with nonlinear least-squares regression to eq 7, or the standard deviation of the slope of the linear van't Hoff plot. Reported errors in $T\Delta S$ are standard deviations. Dashes (−) are shown where T_H and T_S data are not relevant because no heat capacity change was observed. No 11F8 denaturation was detected by CD over the temperature range 5−35 °C.

ometry of salt release (*52*). The larger the stoichiometry of salt release, the larger the thermodynamic impact of the polyelectrolyte effect. Unfavorable entropies accompanying 11F8 binding to noncognate sequences are larger than those observed for 11F8·**WT**. To test the hypothesis that this trend results from reduced ion release in noncognate complexes, the magnitude of the polyelectrolyte effect in 11F8 recognition was evaluated.

The stoichiometries of salt release for 11F8 binding of **WT**, noncognate sequences **LS**, **T7**, T11dU, and ΔdG_4 are presented in Table 1. Representative salt plots are shown in Figure 4. The salt release values for 11F8·**WT** are small and similar to those measured for several RNA binding proteins and other anti-DNA antibodies (*53*−*55*). By contrast, the salt release stoichiometries measured for the noncognate sequences are greater than for **WT**. This trend is similar to what has been observed for other nucleic acid binding proteins, where decreased affinity for noncognate sequences is accompanied by a larger release of cations (*7*, *56*). These results suggest that changes in the polyelectrolyte effect are not responsible for larger unfavorable entropies observed for noncognate recognition relative to **WT**. Recognition of **NS** is accompanied by a significantly larger salt release stoichiometry than observed for **WT** (Table 1). Given that 11F8·**NS** binding is driven by entropy and not accompanied by an enthalpy change, these data suggest that the driving force may result completely from the polyelectrolyte effect, consistent with other nonspecific protein·DNA interactions (*10*, *11*, *57*−*61*).

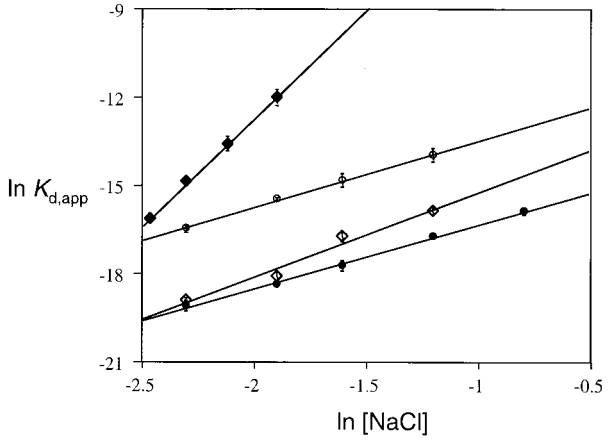

FIGURE 4: Dependence of affinity on buffer [NaCl]. Data for 11F8·**WT** (●), 11F8·**T7** (◇), 11F8·**LS** (○), and 11F8·**NS** (◆) were measured in 20 mM Tris, 85−450 mM NaCl at pH 8, 25 °C.

Cation release data are often interpreted in terms of the number of ionic interactions present in a complex (*52*, *62*):

$$d \ln K_d/dT = z\Psi \ln [MX] \quad (10)$$

where z = number of ion pairs and Ψ = degree of cation condensation per phosphate (ca. 0.7 for ssDNA). However, overall salt release stoichiometry values can also reflect release of anions bound to a protein. The degree to which anions interact with protein surfaces follows the lytotropic series ($H_2SO_4^- \geq OAc^- > > Cl^- > Br^- > > SCN^-$) (*62*,

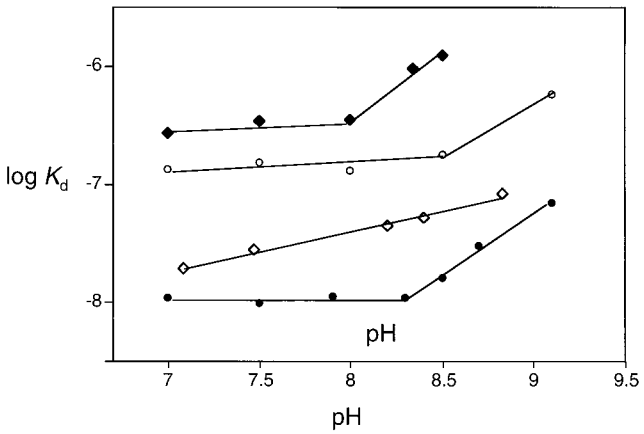

FIGURE 5: Dependence of 11F8 binding on pH for **WT** (●), **T7** (◇), **LS** (○), and **NS** (◆). Data were measured in NaCl buffers (20 mM Tris, 25 °C). **WT**, **LS**, and **T7** data were measured in 150 mM NaCl. **NS** data were measured in 100 mM NaCl.

63). If anion release occurs upon binding, anions that have a lower intrinsic affinity for the protein surface will lead to a smaller ion release stoichiometry than those that interact more strongly. A reduction in ion release stoichiometry is observed for 11F8 binding to **WT** in NaOAc relative to NaCl buffers (1.4 ± 0.1 vs 2.18 ± 0.07), indicating that 11F8·**WT** complexation is accompanied by both anion and cation release. In contrast, no change in salt release stoichiometry is observed for binding to **LS**, **NS**, and T11dU in NaOAc, while **T7** and ΔdG_4 binding may result in slight anion dependence (Table 1).

It is possible that the observed cation release results from conformational changes in **WT** (*64*). Ion release from a conformational change can be distinguished from ion pairing based on the pH dependence of both the affinity and the salt release stoichiometry. Because ion pairing requires a (protonated) basic protein residue, both the salt release stoichiometry and binding affinity should be pH dependent. In contrast, ion release resulting from a rearrangement of the DNA surface should be characterized by a pH-independent salt release stoichiometry. The binding of 11F8 to **WT**, **LS**, ΔdG_4, and **NS** is pH-independent below pH 8.5, above which the affinity for these ligands becomes progressively weaker with increasing pH (Figure 5). Ion release stoichiometry for 11F8·**WT** at pH 9.1 is zero (data not shown), which presumably results from deprotonation of basic protein residues at high pH (*60*, *65*). Similar results were obtained for 11F8·**LS** and 11F8·ΔdG_4 (data not shown). Collectively, these data are consistent with ion pair formation as the source of the observed cation release. In contrast to **WT**, **T7** salt release stoichiometry is not reduced at high pH, although the affinity does vary (linearly) with pH. These data suggest that conformational changes may contribute to the salt release observed for 11F8·**T7**, although similar results for nonspecific binding of the *lac* repressor have been interpreted to reflect ion-pairing resulting from protonation of basic residues that occurs concomitantly with binding (*60*). Regardless, the pH sensitivity of 11F8·**T7** suggests that the same process is not responsible for salt release in both complexes and that the mode of binding is altered for **T7** relative to **WT**.

Since acetate anions are highly excluded from macromolecular surfaces (*63*, *66*), they are unlikely to be site-bound at protein or DNA sites and then released into solution upon protein·DNA complexation. Hence, any contribution of anion release to salt release stoichiometries in NaOAc buffers should be small. Therefore, salt release stoichiometries in NaOAc can be interpreted as reflecting only cation release. The number of possible ion pairs formed in each 11F8·DNA complex can be estimated according to eq 10, which corrects the salt release stoichiometry for the thermodynamic degree of cation condensation per phosphate (*67*) (0.7 for ssDNA). Binding studies in NaOAc buffer suggest that 2 ion-pairs form in the 11F8·**WT** complex, 3 form in the 11F8·**LS** and 11F8·ΔdG_4 complexes, and 10 ion-pairs are formed upon binding **NS**. Taken together, these salt dependence data suggest that the polyelectrolyte effect provides only a small energetic contribution to 11F8·**WT** affinity, consistent with the observed unfavorable entropy change (Table 2). Increased cation release accompanies lower affinity binding to noncognate sequences **LS**, **T7**, ΔdG_4, and T11dU. Since binding of these sequences occurs with an even more unfavorable entropy change than is observed for **WT**, the entropic bonus from increased salt release is not sufficient to compensate for the higher entropic costs associated with noncognate recognition. Presumably, higher entropic costs could result from changes in solvation or differences in conformational or vibrational degrees of freedom for noncognate complexes versus 11F8·**WT**.

Polarity Experiments. Binding of **WT** and noncognate sequences is enthalpically driven over the physiological temperature range. Intermolecular contacts like van der Waals interactions and direct protein·DNA hydrogen bonds are traditionally associated with favorable enthalpies and presumably require desolvation, or water release, at the binding interface (*68*). However, water release is generally associated with favorable changes in entropy at room temperature (*69*) that are not observed for 11F8·**WT** or 11F8·noncognate complexes. To further understand the processes driving complexation, a series of experiments were conducted to investigate the impact of bulk solution polarity changes in 11F8·DNA recognition.

To test whether the driving force for 11F8·**WT** binding is provided by the hydrophobic effect, the sensitivity of binding affinity to addition of nonpolar solvents was investigated. Binding titrations were carried out in buffers containing up to 28% w/v added methanol, ethanol, 1-propanol, or glycerol. Addition of nonpolar solvents reduces the energetic contribution of the hydrophobic effect by stabilizing interactions between bulk solvent and hydrophobic surfaces in free 11F8 and **WT**. Consequently, if the hydrophobic effect drives binding, the energy difference between bound and unbound states is reduced in the presence of nonpolar solvents. The data in Table 3 and Figure 6 demonstrate that binding of **WT** is reduced by addition of each solvent, which suggests that the hydrophobic effect stabilizes the 11F8·**WT** complex. High concentrations of glycerol or other nonaqueous solvents can decrease the degree of cation condensation on DNA structure (*70*). To determine if the observed affinity decreases with added solvents result from changes in salt release, 11F8·**WT** NaCl release stoichiometry was measured in the presence of added glycerol (28% w/v). Observed salt release stoichiometries were indistinguishable from those measured in the absence of added solvent, indicating that the observed affinity

Table 3: Sensitivity of 11F8 Binding Affinity to Osmotic Stress and Solvent Polarity[a]

sequence	osmolyte	plot slope: ln K_d vs [O]	plot slope: ln K_d vs ϵ
WT	glycerol	0.32 ± 0.03	−0.24 ± 0.02
	methanol	0.27 ± 0.02	−0.25 ± 0.02
	ethanol	0.55 ± 0.07	−0.24 ± 0.03
	1-propanol	1.04 ± 0.04	−0.27 ± 0.05
T7	glycerol	0.37 ± 0.02	−0.25 ± 0.02
	1-propanol	1.29 ± 0.04	−0.35 ± 0.01
LS	glycerol	0.42 ± 0.02	−0.29 ± 0.02
	1-propanol	1.38 ± 0.05	−0.35 ± 0.02
T11dU	glycerol	0.32 ± 0.03	−0.22 ± 0.03
	methanol	0.29 ± 0.01	−0.22 ± 0.01
	ethanol	0.45 ± 0.02	−0.29 ± 0.01
	1-propanol	0.98 ± 0.04	−0.27 ± 0.01
ΔdG_4	glycerol	0.30 ± 0.06	−0.20 ± 0.02
	methanol	0.29 ± 0.02	−0.28 ± 0.07
	ethanol	0.47 ± 0.02	−0.30 ± 0.01
	1-propanol	1.08 ± 0.05	−0.27 ± 0.02
NS	glycerol	0.05 ± 0.03	−0.05 ± 0.02

[a] Data for all sequences were measured in 20 mM Tris, 300 mM NaCl, pH 8, 20 °C, except for **NS** measurements, which used 20 mM Tris, 100 mM NaCl, pH 8, 20 °C. Data shown are the slopes of the plot of ln K_d vs either bulk solution dielectric constant (ϵ) or osmolal concentration, [O]. No changes in 11F8 conformation were detected by CD over the polarity range used in these experiments.

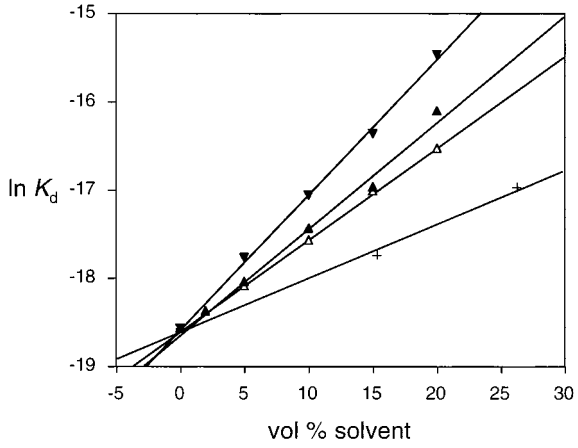

FIGURE 6: Dependence of 11F8·**WT** affinity on addition of nonpolar solvents. Data were measured at 20 °C in 20 mM Tris, pH 8, 300 mM NaCl in the presence of either glycerol (+), methanol (△), ethanol (▲), or 1-propanol (▼) (up to 25% v/v).

decreases do not result from changes in the polyelectrolyte effect (data not shown).

Nonaqueous solvents reduce bulk water activity as well as solution polarity. Hence, it is possible that the observed affinity decreases caused by added solvent could result from changes in osmotic stress rather than bulk solution polarity. Previous studies of protein·dsDNA and antibody·antigen binding have interpreted affinity decreases with increasing osmotic stress to reflect water uptake concomitant with binding (*71*, *72*). If changes in osmotic stress are primarily responsible for the observed affinity decreases, the dependence of affinity on solution [osmolal] should be similar for each solvent (*73*−*75*). However, if polarity is the primary contributor to the observed affinity decreases, the dependence of affinity on bulk solution polarity should be independent of solvent choice. As shown in Figure 7a and Table 3, the dependence of 11F8·**WT** affinity on osmolal concentration varies widely between solvents, indicating that osmolal

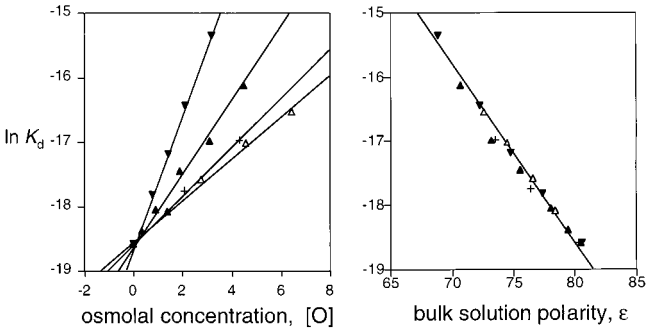

FIGURE 7: Dependence of 11F8·**WT** affinity on added nonpolar solvent, presented as a function of (a) osmolal concentration and (b) bulk solution dielectric constant. Data were measured at 20 °C in 20 mM Tris, pH 8, 300 mM NaCl in the presence of up to 25% w/v of either glycerol (+), methanol (△), ethanol (▲), or 1-propanol (▼). Dielectric constant values represent bulk solution and are therefore normalized for polarity differences between individual solvents.

concentration is not the only variable affecting affinity. However, the dependence of 11F8·**WT** affinity on bulk solution polarity is indistinguishable for the four solvents (Figure 7b; Table 3). Taken together, these suggest that the primary source of the decreased affinity with nonpolar solvent addition is a reduction in bulk solution polarity, rather than changes in osmotic stress.

Changes in polarity might be expected to impact hydrogen-bonding strength in addition to reducing favorable driving force from the hydrophobic effect. However, in systems where hydrogen bonding provides the primary driving force for complexation, reductions in buffer polarity lead to increases in affinity (*76*, *77*), in contrast to what is observed for 11F8·**WT** binding. Hence, the sensitivity of 11F8·**WT** affinity to polarity changes suggests that hydrogen bonding is neither the largest thermodynamic driving force for 11F8·**WT** binding nor the primary source of the observed favorable enthalpic driving force. Instead, the enthalpic driving force must be provided by hydrophobic interactions between nonpolar surfaces on 11F8 and **WT** surfaces, stacking of aromatic 11F8 side chains with **WT** nucleotide bases, and desolvation at the binding interface.

Interactions between hydrophobic surfaces that result in water release have traditionally been associated with favorable entropy changes (*69*). However, recent theoretical and empirical studies have suggested that the hydrophobic effect may be enthalpy-driven, depending on surface topography (*78*−*83*). Enthalpy-driven "nonclassical" hydrophobic interactions have recently been assigned as the driving force for several protein·carbohydrate (*84*, *85*), membrane·peptide (*86*−*89*), and host·guest systems (*90*−*92*). The sensitivity of 11F8·**WT** binding to polarity, coupled with the enthalpic driving force, argues that 11F8·**WT** interaction is driven by a similar effect. Since the entropy changes accompanying desolvation of nonclassical hydrophobic surfaces may be small, the apparent insensitivity of 11F8·**WT** binding to osmotic stress does not preclude water release upon binding.

The sensitivity of 11F8·**LS** and 11F8·**T7** affinity to addition of solvents is greater than that observed for 11F8·**WT** (Table 3). These results suggest that the hydrophobic surface area enclosed in these complexes may be larger than for 11F8·**WT**, and could be responsible for some of the observed higher favorable enthalpy changes. In contrast, the

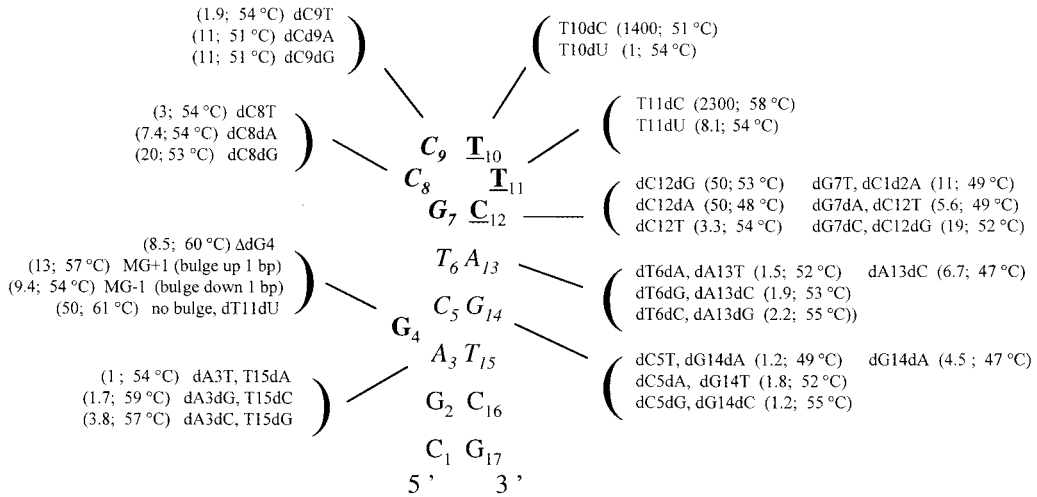

FIGURE 8: **WT** mutants and proposed **WT** recognition surface based on footprinting experiments. T_m and relative K_d values are shown in parentheses. Relative K_d values are normalized against **WT**. Each affinity measurement was conducted at least 3 times, affording standard error ≤30% of the average K_d. Bases that directly contact 11F8 (T_{10},T_{11}, dC_{12}) are shown underlined in boldface type. Other bases modulate recognition by affecting free ligand conformation (dG_4, shown in boldface), stem secondary structure (T_6-dA_{13}, dC_5-dG_{14}, and dA_3-T_{15}, shown in italics), or both free ligand conformation and mode of binding (dG_7, dC_8, and dC_9, shown in boldface italics).

sensitivity of 11F8·T11dU and 11F8·ΔdG_4 affinity to addition of solvents is similar to that observed for 11F8·**WT** (Table 3). These data suggest that the hydrophobic driving force for 11F8·T11dU and 11F8·ΔdG_4 is similar to that present in 11F8·**WT** and that increases in hydrophobic effect involvement are not the source of the observed higher enthalpy changes for these complexes relative to 11F8·**WT**.

Significant differences in the both the enthalpy and entropy changes, sensitivity to polarity, and anion and cation release associated with 11F8 binding to **WT** relative to the variant sequences indicate that the sequences are recognized in different ways. These differences may be due to DNA binding at a slightly altered binding site within the 11F8 complementarity determining regions (CDRs), or from differing interactions made possible by conformational changes in 11F8 or DNA surfaces. To investigate possible conformational changes, CD spectra of 11F8, DNA, and 11F8·DNA complexes were measured from 200 to 300 nm. The spectra of the 11F8 complexes were compared to the sum of the spectra of unbound 11F8 and DNA. No significant differences between the spectra of 11F8 complexes and free 11F8 and DNA were observed in the regions corresponding to DNA (220−300 nm) or protein (200−240 nm) (*93*) for 11F8·**WT**, 11F8·**LS**, 11F8·**T7**, and 11F8·ΔdG_4 complexes (data not shown). These data suggest that no large-scale structural changes occur upon 11F8 binding of these sequences. This result does not preclude all conformational adjustments, however, since many conformational changes observed for antibody−antigen complexes are reorientations of side chain conformation or CDR alignment (*94*, *95*) that CD may not detect. In contrast, a 30% decrease in the magnitude of the band at 220 nm occurs for 11F8·**NS** relative to free 11F8 and **NS** (data not shown). This result suggests that the different binding mode exhibited for 11F8·**NS** recognition may require much larger alterations in 11F8 or DNA conformation.

Mapping the DNA Recognition Surface. Specific DNA binding by 11F8 is achieved only when the recognition elements on **WT** are presented within a well-defined secondary structure. Fluorescence quenching and chemical footprinting experiments on **WT** and several mutant sequences were conducted to determine which nucleotides directly contact the protein (sequence specificity) and which nucleotides contribute to binding through the secondary structure (conformational specificity). Previous studies have demonstrated that T_{10} and T_{11} provide critical sequence-dependent recognition contacts for 11F8 (*33*). Decreased affinity for **LS** and ΔdG_4 suggests that both the stem and bulge are important for 11F8 recognition. Consequently, the sequence-dependent role for the methyl groups of T_{10} and T_{11}, the base size at positions 8 and 9, and the sequence of the stem and the bulge were investigated by systematically altering each base or base pair from dA_3 to T_{15} (Figure 8).

Nucleotides Protected from $KMnO_4$ Modification in the Presence of 11F8. Potassium permanganate selectively oxidizes the C5−C6 double bond of thymine bases that are not Watson−Crick hydrogen-bonded (*96*, *97*). In the presence of protein, the magnitude of reactivity at individual thymine bases can be altered at positions that are contacted by the protein or which undergo a protein-dependent conformational change. $KMnO_4$ footprinting of the 11F8·**WT** complex shows strong protection of T_{10} and T_{11}, somewhat weaker protection of T_{15}, and slightly increased reactivity of T_6 (*33*). Differences in this protection pattern for mutant ligands can be used to assess changes in the interaction with 11F8. Changes in reactivity at these bases in the absence of 11F8 reflect differences in free DNA conformation relative to **WT**.

To probe the role of the thymine methyl group, T_{10} and T_{11} were each replaced with dU. Substitution of T_{10} with dU does not alter the binding affinity or the $KMnO_4$ protection pattern in the presence or absence of 11F8. In addition, both the temperature dependence and salt release stoichiometry measured for T10dU are identical to **WT** (data not shown). These data suggest that the T_{10} methyl group does not contribute to recognition. However, the T11dU mutant binds 8-fold weaker than **WT**, and the pattern of $KMnO_4$ protection in the 11F8·T11dU complex shows decreased protection at T_{10} and dU_{11} relative to the 11F8·**WT** complex (Figure 9). Moreover, unlike **WT**, the binding

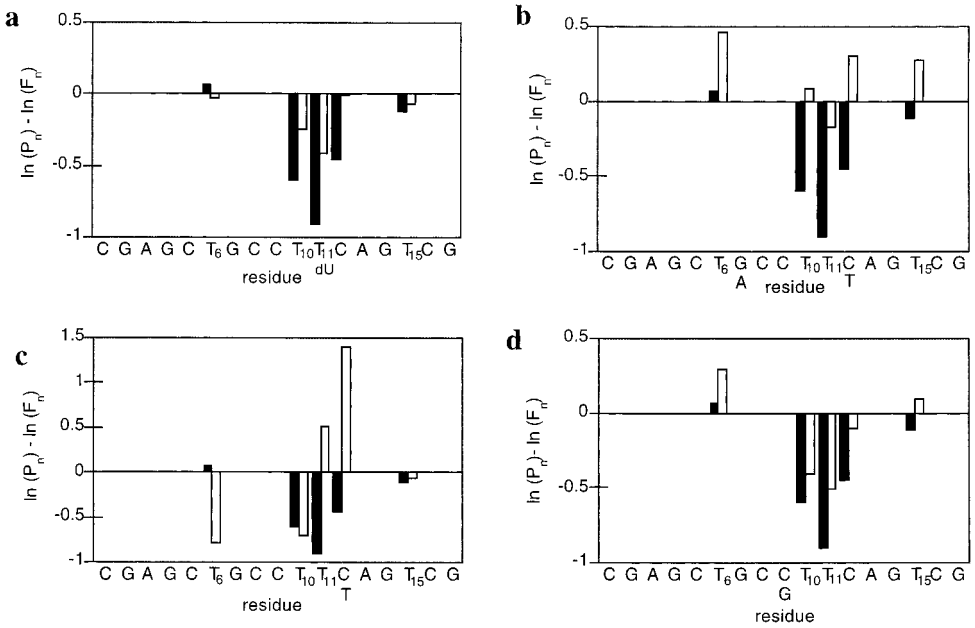

FIGURE 9: Quantification of representative $KMnO_4$ protection footprinting for 11F8 in complex with (a) **WT** and dT11dU, (b) **WT** and (dG7dA, dC12dT), (c) **WT** and dC12dT, and (d) **WT** and dC9dG. Black bars = **WT**, white bars = mutant sequence. The difference in strand cleavage is represented by bars and is calculated by subtracting the logarithm of the probability of cleavage at each position in the free DNA (F_n) from the same position in the complex (P_n) (*43*). A larger negative value of $\ln(P_n/F_n)$ indicates greater protection from $KMnO_4$ oxidation.

of T11dU is not accompanied by a heat capacity change. These data indicate that the T_{11} methyl group is important for recognition and may directly contact 11F8 (Figure 8).

Nucleotide dC_{12} is also susceptible to oxidation by $KMnO_4$ in the absence of 11F8 and shows decreased $KMnO_4$ reactivity in the presence of protein, suggesting possible 11F8 contacts at this position. To investigate how dC_{12} contributes to binding, dG_7-dC_{12} base pair mutants and individual base substitutions of dC_{12} were studied. Substituting dG_7-dC_{12} with T_7-dA_{12}, dA_7-T_{12}, or dC_7-dG_{12} decreases affinity 6−20-fold (Figure 8). These mutants are not accompanied by significant protection of T_{10} or T_{11} from $KMnO_4$ oxidation in the presence of 11F8 (Figure 9b). In addition, all dC_{12} point mutations (dC12dG, dC12dA, and dC12T) bind weakly to 11F8, and show increased reactivity of T_{10}, T_{11}, and T_{15} in the absence of protein, as well as altered $KMnO_4$ protection patterns in the presence of 11F8 (Figure 9c). Taken together, these studies suggest that dC_{12} is important for recognition by 11F8, probably in the context of a G−C base pair.

Secondary Structure Nucleotides. Footprinting experiments with monopersulfate/KBr, which specifically modifies single-stranded dC bases (*98*), show no difference in the reactivity of dC_8 and dC_9 in the presence or absence of 11F8, suggesting that these nucleotides may not be directly contacted. Conservative pyrimidine substitutions (dC9T and dC10T) bind ≤3-fold weaker than **WT**, and their reactivity to $KMnO_4$ is nearly identical to **WT** in the presence of 11F8. In contrast, purine substitutions bind 10−20-fold more weakly than **WT**, and show altered reactivity of T_{10}, T_{11}, and dC_{12} to $KMnO_4$ in the presence or absence of 11F8, relative to **WT** (Figure 9d). Losses in affinity as well as decreased protection of T_{10}, T_{11}, and dC_{12} presumably reflect the steric effects of a bulkier base present in the loop and suggest that a pyrimidine is required at positions 8 and 9 to provide an optimal loop geometry for binding.

The importance of presenting T_{10}, T_{11}, and dC_{12} in a well-defined secondary structure is suggested by the fact that **LS** binds 10-fold weaker than **WT**. To investigate the role of the stem duplex in 11F8 recognition, mutants that individually changed three base pairs in the stem (T_6-dA_{13}, dC_5-dG_{14}, dA_3-T_{15}) to all other canonical base pair combinations were studied (Figure 8). Binding affinities for all mutants are within 4-fold of **WT**, and no significant changes to the $KMnO_4$ modification patterns are observed either in the absence or in the presence of 11F8. These data suggest that the stem duplex serves only to provide the necessary secondary structure for recognition by 11F8.

Conformational Effects of the Bulge. Removing dG_4 from **WT** decreases affinity 9-fold without significant alteration of the $KMnO_4$ footprint in the presence of 11F8. However, changing the dG_4 to dC has no impact on the thermodynamics of binding. Footprinting the 11F8·**WT** complex with DMS and DEPC, both purine-specific reagents, shows no protection of dG_4 from modification (data not shown). Taken together, these data suggest that the bulge at position 4 contributes to affinity but does not directly contact 11F8. Studies of bulged DNA duplexes demonstrate that, depending on its conformation, a bulged nucleotide can exert significant conformational effects on surrounding nucleotides (*99*, *100*). Significant modification by DMS at dG_4, both in the presence and in the absence of 11F8, suggests that this nucleotide extends out into solution and does not stack with the bases in the helix. Consequently, the primary structural contribution of the bulge is expected to be a destabilization of helical stacking, resulting in a more "open" stem conformation (*15*, *101*). Consistent with this interpretation, the free energy of melting for ΔdG_4 is 2 kcal higher than for **WT** at 150 mM NaCl. A correlation between helix stability and 11F8 affinity is suggested by the observation that the differences in free energy of melting of **WT** and ΔdG_4 ($\Delta\Delta G_{melting}$) and free energies of binding ($\Delta\Delta G_{binding}$) are within error for the two

sequences at 1 M NaCl, where the effects of differences in salt release stoichiometry are negligible ($\Delta\Delta G_{binding} = 1.6$ kcal/mol; $\Delta\Delta G_{melting} = 1.7 \pm 0.3$ kcal/mol).

DISCUSSION

*Sequence-Specific Recognition of **WT***. Binding of **WT** is opposed by entropy, is driven by enthalpy, and is accompanied by a negative heat capacity change. Our data suggest that the favorable enthalpy change derives in large part from the nonclassical hydrophobic effect. This effect differs from the classical understanding of the hydrophobic effect, which is derived from measuring the transfer of small nonpolar solutes from water to nonaqeuous solvent (*69*). However, recent theoretical analyses have suggested that the classical hydrophobic effect may not apply to systems where hydrophobic surface topography does not resemble the small concave surface of model solutes (*78*, *81*, *102*, *103*). For example, molecular dynamics calculations predict that planar or concave nonpolar surfaces, or those adjacent to polar or charged surfaces, are solvated by nonclathrate water structures that are incompletely hydrogen-bonded (*79*, *83*, *104*, *105*). Desolvation of these surfaces upon binding results in a significant favorable enthalpic driving force as water molecules become fully hydrogen-bonded in bulk solvent (*78*, *79*). This phenomenon is believed to drive the binding of several protein·carbohydrate (*79*, *84*, *85*), protein·ligand (*106*−*108*), membrane·peptide (*86*−*89*), membrane·ligand (*109*, *110*), and many host·guest recognition systems (*91*, *92*). In addition, cyclophane·guest interactions, which have been proposed as models for hydrophobic interactions in both antibody·antigen and protein·nucleic acid complexes, show favorable enthalpies, unfavorable entropies, and sensitivity to solution polarity similar to those observed for 11F8·**WT** (*90*, *111*).

Enthalpy and entropy values measured for 11F8·**WT** are similar to those reported for high-affinity sequence-specific recognition of RNA. For example, R17 coat protein binds to the loop region of a bulged RNA hairpin with favorable enthalpy ($\Delta H = -19$ kcal/mol) and unfavorable entropy ($T\Delta S = -8.9$ kcal/mol) (*45*, *112*). Human U1A protein recognizes a seven base-long hairpin loop with comparable thermodynamic parameters including a negative heat capacity change [$\Delta H = -17$ kcal/mol; $\Delta C_p = -1.4$ kcal/(mol·K)] (*113*). These observations suggest that 11F8·**WT** recognition may have more in common with sequence-specific protein·RNA systems than most protein·dsDNA systems. In part, similarities may arise because both RNA binding proteins and 11F8 recognize their target ligands in the context of nucleic acid secondary structure. In both cases, secondary structure promotes high-affinity recognition by restraining conformational flexibility prior to complexation, thus reducing the losses in conformational entropy otherwise associated with binding single-stranded nucleic acids.

Nonspecific 11F8 Recognition. Unlike the 11F8·**WT** complex, 11F8 recognition of **NS** is driven completely by the polyelectrolyte effect. $KMnO_4$ modification of 11F8·**NS** shows no significant protection of thymine, suggesting that no intimate contacts are made between 11F8 and DNA bases. Consistent with these data, and in contrast to **WT** binding, 11F8·**NS** recognition is not accompanied by a change in enthalpy or heat capacity. The different thermodynamic driving force(s) for 11F8 recognition of **NS** and **WT** demonstrate(s) the ability of 11F8 to adapt its mode of binding to the available DNA surface, as has been observed for other nucleic acid binding proteins (*10*, *14*, *114*, *115*). The most energetically favorable set of 11F8 interactions is defined by the high-affinity 11F8·**WT** complex. In the absence of the **WT** recognition surface, 11F8 chooses the next most favorable set of interactions, which for 11F8·**NS** involves extensive electrostatic interactions with the phosphate backbone.

Binding of Noncognate Sequences. Binding of noncognate sequences is accompanied by pronounced increases in favorable enthalpy and unfavorable entropy relative to 11F8·**WT**. It is possible that these differences result from alterations in the thermodynamic signature of the hydrophobic effect. Dill has recently proposed that the thermodynamic signature of the hydrophobic effect is a continuum that varies from purely entropy-driven with a large negative heat capacity change to purely enthalpy-driven with opposing entropy and no heat capacity change (*78*). In this case, the magnitudes of the enthalpy and entropy changes are determined by the pattern of hydration of hydrophobic surfaces enclosed in the complex. Since each noncognate sequence presents a different recognition surface than **WT**, the DNA hydration pattern should be altered for each sequence. According to this model, the increases in enthalpy and entropy upon binding noncognate sequences may reflect decreases in the degree of ordering of hydrating water molecules relative to **WT**.

Alternatively, it is possible that some of the differences in binding thermodynamics could result from (small) changes in DNA contacts in the noncognate complexes. While sensitivity to polarity and the pattern of $KMnO_4$ protection show that both the noncognate and **WT** complexes make similar 11F8·DNA contacts, some alterations are evident. For example, $KMnO_4$ protection experiments show that dC_{12} is not protected in the 11F8·T11dU complex, indicating that the substitution results in changes in the binding of adjacent nucleotides. Similarly, the sensitivity of the noncognate complexes to increasing [MX] suggests that a larger number of ionic contacts are present in noncognate complexes than in 11F8·**WT**. However, the structural differences are relatively subtle and in most cases involve reduced contacts at key residues. Consequently, it is unlikely that these differences account significantly for the large increases in favorable enthalpy observed for noncognate recognition.

The change in enthalpy for **WT** and noncognate recognition is linearly correlated with the change in entropy (Figure 10). Similar linear relationships are documented in a wide variety of systems and are believed to characterize processes in which solvation changes play an important role in binding (*116*−*118*). This interpretation is consistent with Dill's model of the hydrophobic effect in which the thermodynamic signature of desolvation shifts from entropic to enthalpic depending on the pattern of hydration. For 11F8, increases in favorable enthalpy are offset by unfavorable entropy, and it is this effect that results in specificity for **WT**. A similar phenomenon has been observed for host·guest interactions and is thought to reflect conformational adaptation to maximize favorable interaction in the complex (*92*, *119*). Thus, the observed enthalpy−entropy compensation is consistent with both structural adaptation in noncognate

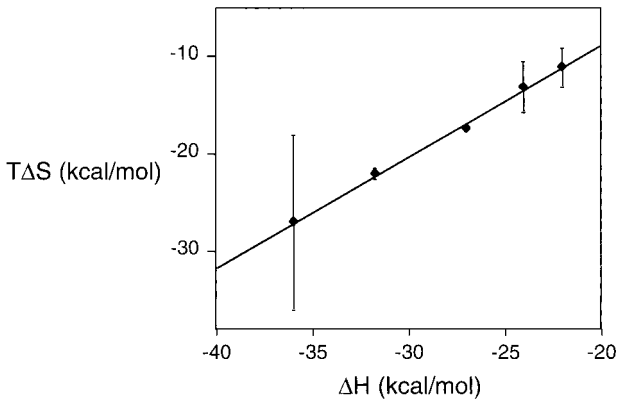

FIGURE 10: Enthalpy−entropy compensation for 11F8 binding. Data included are values obtained for **WT**, **T7**, ΔdG_4, dT11dU, and **LS**. The equation of best fit is $T\Delta S = 1.14(\Delta H) + 13.99$; $R^2 = 0.998$. Error bars shown for $T\Delta S°_{obs}$ are propagated from errors in $\Delta H°_{obs}$ and $\Delta G°_{obs}$.

complexes and the key role of the hydrophobic effect in 11F8 binding.

REFERENCES

1. von Hippel, P. H., and Berg, O. G. (1986) *Proc. Natl. Acad. Sci. U.S.A. 83*, 1608−1612.
2. von Hippel, P. H. (1994) *Science 263*, 769−770.
3. Ha, J.-H., Spolar, R. S., and Record, M. T. J. (1989) *J. Mol. Biol. 209*, 801−816.
4. Oda, M., Furukawa, K., Ogata, K., Sarai, A., and Nakamura, H. (1998) *J. Mol. Biol. 276*, 571−590.
5. Merabet, E., and Ackers, G. K. (1995) *Biochemistry 34*, 8554−8563.
6. Ladbury, J. E., Wright, J. G., Sturtevant, J. M., and Sigler, P. B. (1994) *J. Mol. Biol. 238*, 669−681.
7. Hard, T., and Lundback, T. (1996) *Biophys. Chem. 62*, 121−139.
8. Janin, J. (1995) *Proteins: Struct., Funct., Genet. 21*, 30−39.
9. Revzin, A. (1990) *Biology of Nonspecific DNA−Protein Interactions*, pp 33−70, CRC Press, Boca Raton, FL.
10. Jen-Jacobsen, L. (1997) *Biopolymers 44*, 153−180.
11. McAfee, J. G., Edmondson, S. P., Zegar, I., and Shriver, J. W. (1996) *Biochemistry 35*, 4034−4045.
12. Draper, D. E. (1999) *J. Mol. Biol. 293*, 255−270.
13. Nagai, K. (1996) *Curr. Opin. Struct. Biol. 6*, 53−61.
14. Frankel, A. D., and Smith, C. A. (1998) *Cell 92*, 149−151.
15. Lustig, B., Bahar, I., and Jernigan, R. L. (1998) *Nucleic Acids Res. 26*, 5212−5217.
16. Kowalczykowski, S. C., Lonberg, N., Newport, J. W., and von Hippel, P. H. (1981) *J. Mol. Biol. 145*, 75−104.
17. Newport, J. W., Lonberg, N., Kowalczykowski, S. C., and von Hippel, P. H. (1981) *J. Mol. Biol. 145*, 105−121.
18. Kowalczykowski, S. C., Bear, D., and von Hippel, P. H. (1981) in *Nucleic Acids* (Boyer, P. D., Ed.) Academic Press, Inc., London.
19. Lohman, T. M., and Ferrari, M. E. (1994) *Annu. Rev. Biochem. 63*, 527−570.
20. Casas-Finet, J. R., Khamis, M. I., Maki, A. H., Ruvolo, P. P., and Chase, J. W. (1987) *J. Biol. Chem. 262*, 8574−8583.
21. Khamis, M. I., Casas-Finet, J. R., Maki, A. H., Ruvolo, P. P., and Chase, J. W. (1987) *Biochemistry 26*, 3347−3354.
22. Coleman, J. E., Williams, K. R., King, G. C., Prigodich, R. V., Shamoo, Y., and Konigsberg, W. H. (1986) *J. Cell. Biochem. 32*, 305−326.
23. Overman, L. B., Bujalowski, W., and Lohman, T. M. (1988) *Biochemistry 27*, 456−471.
24. Flavin, M., and Strauss, F. (1991) *DNA Cell Biol. 10*, 113−118.
25. Haas, S., Steplewski, A., Siracusa, L. D., Amini, S., and Khalili, K. (1995) *J. Biol. Chem. 270*, 12503−12510.
26. Habiger, C., Stelzer, G., Schwarz, U., and Winnacker, E.-L. (1992) *J. Virol. 66*, 5988−5998.
27. Menon, R. K., Cheng, H., and Singh, M. (1997) *Mol. Endocrinol. 11*, 1291−1304.
28. Nambiar, A., Swamynathan, S. K., Kandala, J. C., and Guntaka, R. (1998) *J. Virol. 72*, 900−909.
29. Katz, J. B., Limpanasithikul, W., and Diamond, B. (1994) *J. Exp. Med. 180*, 925−932.
30. Waer, M. (1990) *Clin. Rheumatol. Suppl. 1 9*, 111−114.
31. Isenberg, D. A., Ehrenstein, M. R., Longhurst, C., and Kalsi, J. K. (1994) *Arthritis Rheum. 37*, 169−180.
32. Ben-Chetrit, E., Eilat, D., and Ben-Sasson, S. A. (1988) *Immunology 65*, 479−485.
33. Stevens, S. Y., and Glick, G. D. (1999) *Biochemistry 38*, 560−568.
34. Swanson, P. C., Ackroyd, C., and Glick, G. D. (1996) *Biochemistry 35*, 1624−1633.
35. Mach, H., Middaugh, C. R., and Lewis, R. V. (1992) *Anal. Biochem 200*, 74−80.
36. Fasman, G. D. (1977) *CRC Handbook of Biochemistry and Molecular Biology*, 3rd ed., Vol. 1, p 589, CRC Press, Cleveland, OH.
37. Birdsall, B., King, R. W., Wheeler, M. R., Lewis, C. A., Goode, S. R., Dunlap, R. B., and Roberts, G. C. K. (1983) *Anal. Biochem. 132*, 353−361.
38. Lohman, T. M., and Mascotti, D. P. (1992) *Methods Enzymol. 212*, 424−458.
39. Baldwin, R. L. (1986) *Proc. Natl. Acad. Sci. U.S.A. 83*, 8069−8072.
40. Hewitt, G. F. (1970) *CRC Handbook of Chemistry and Physics*, CRC Press, Boca Raton, FL.
41. Akerlof, G. (1932) *J. Am. Chem. Soc. 54*, 4125−4139.
42. Swanson, P. C., Cooper, B. C., and Glick, G. D. (1994) *J. Immunol. 152*, 2601−2612.
43. Rhodes, D. (1988) in *Protein Function: A Practical Approach* (Creighton, T. E., Ed.) IRL Press, Oxford.
44. Kurumizaka, H., Kanke, F., Matsumoto, U., and Shindo, H. (1992) *Arch. Biochem. Biophys. 295*, 297−301.
45. Hall, K. B. (1994) *Biochemistry 33*, 10076−10088.
46. Uhlenbeck, O. C., Carey, J., Romaniuk, P. J., Lowary, P. T., and Beckett, D. (1983) *J. Biomol. Struct. Dyn. 1*, 539−551.
47. Bujalowski, W., and Lohman, T. M. (1989) *J. Mol. Biol. 207*, 269−288.
48. Alma, N. C. M., Harmsen, B. J. M., De Jong, E. A. M., van der Ven, J., and Hilbers, C. W. (1983) *J. Mol. Biol. 163*, 47−62.
49. Komissarov, A. A., and Deutscher, S. L. (1999) *Biochemistry 38*, 14631−14637.
50. Brun, F., Toulme, J.-J., and Helene, C. (1975) *Biochemistry 14*, 558−563.
51. Helene, C., and Lancelot, G. (1982) *Prog. Biophys. Mol. Biol. 39*, 1−68.
52. Record, M. T. J., Lohman, T. M., and deHaseth, P. (1976) *J. Mol. Biol. 107*, 145−158.
53. Lee, J. S., Dombroski, D. F., and Mosmann, T. R. (1982) *Biochemistry 21*, 4940−4945.
54. Tanha, J., and Lee, J. S. (1997) *Nucleic Acids Res. 25*, 1442−1449.
55. Slice, L. W., Codner, E., Antelman, D., Holly, M., Wegrzynski, B., Wang, J., Toome, V., Hsu, M.-C., and Nalin, C. M. (1992) *Biochemistry 31*, 12062−12068.
56. Frank, D. E., Saecker, R. M., Bond, J. P., Capp, M. W., Tsodikov, O. V., Melcher, S. E., Levandoski, M. M., and Record, M. T. J. (1997) *J. Mol. Biol. 267*, 1186−1206.
57. Latt, S. A., and Sober, H. A. (1967) *Biochemistry 6*, 3293−3306.
58. Lohman, T. M., de Haseth, P. L., and Record, M. T. J. (1980) *Biochemistry 19*, 3522−3530.
59. deHaseth, P. L., Lohman, T. R., and Record, M. T. J. (1977) *Biochemistry 16*, 4783−4790.
60. Takeda, Y., Ross, P. D., and Mudd, C. P. (1992) *Proc. Natl. Acad. Sci. U.S.A. 89*, 8180−8184.
61. Record, M. T. J., Anderson, C. F., and Lohman, T. M. (1978) *Q. Rev. Biophys. 11*, 103−178.

62. Collins, K. D., and Washabaugh, M. W. (1985) *Q. Rev. Biophys. 18*, 323−422.
63. Misra, V. K., Hecht, J. L., Sharp, K. A., Friedman, R. A., and Honig, B. (1994) *J. Mol. Biol. 238*, 264−280.
64. Overman, L. B., and Lohman, T. M. (1994) *J. Mol. Biol. 236*, 165−178.
65. Cacace, M. G., Landau, E. M., and Ramsden, J. J. (1997) *Q. Rev. Biophys. 30*, 241−277.
66. Ha, J.-H. (1990) Ph.D. Thesis, University of Wisconsin, Madison.
67. Davies, D. R., Padlan, E. A., and Sheriff, S. (1990) *Annu. Rev. Biochem. 59*, 439−473.
68. Tanford, C. (1980) *The Hydrophobic Effect: Formation of Micelles and Biological Membranes*, John Wiley and Sons, New York.
69. Spink, C. H., and Chaires, J. B. (1999) *Biochemistry 38*, 496−508.
70. Robinson, C. R., and Sligar, S. G. (1996) *Protein Sci. 5*, 2119−2124.
71. Colombo, M. F., Rau, D. C., and Parsegian, V. A. (1992) *Science 256*, 655−659.
72. Robinson, C. R., and Sligar, S. G. (1995) *Methods Enzymol. 259*, 395−427.
73. Parsegian, V. A., Rand, R. P., and Rau, D. C. (1995) *Methods Enzymol. 259*, 43−94.
74. Vossen, K. M., Wolz, R., Daugherty, M. A., and Fried, M. G. (1997) *Biochemistry 36*, 11640−11647.
75. Adrian, J. C. J., and Wilcox, C. S. (1991) *J. Am. Chem. Soc. 113*, 678−680.
76. Sneddon, S. F., Tobias, D. J., and Brooks, C. L. I. (1989) *J. Mol. Biol. 209*, 817−820.
77. Southall, N. T., and Dill, K. A. (2000) *J. Phys. Chem. B 104*, 1326−1331.
78. Lemieux, R. U. (1996) *Acc. Chem. Res. 29*, 373−380.
79. Isbister, B. D., St. Hilaire, P. M., and Toone, E. J. (1995) *J. Am. Chem. Soc. 117*, 12877−12878.
80. Wallqvist, A., and Berne, B. J. (1995) *J. Phys. Chem. 99*, 2885−2892.
81. Lee, C. Y., McCammon, J. A., and Rossky, P. J. (1984) *J. Chem. Phys 80*, 4448−4455.
82. Cheng, Y.-K., Sheu, W.-S., and Rossky, P. J. (1999) *Biophys. J. 76*, 1734−1743.
83. Chervenak, M. C., and Toone, E. J. (1994) *J. Am. Chem. Soc. 116*, 10533−10539.
84. Williams, B. A., Chervenak, M. C., and Toone, E. J. (1992) *J. Biol. Chem. 267*, 22907−22911.
85. Wong, T. C., and Gao, X. (1998) *Biopolymers 45*, 395−403.
86. Wieprecht, T., Beyermann, M. W., and Seelig, J. (1999) *Biochemistry 38*, 10377−10387.
87. Mozsolits, H., Lee, T.-H., Wirth, H.-J., Perlmutter, P., and Aguilar, M. I. (1999) *Biophys. J. 77*, 1428−1444.
88. Gazzara, J. A., Phillips, M. C., Lund-Katz, S., Palgunachari, M. N., Segrest, J. P., Anantharamaiah, G. M., and Snow, J. W. (1997) *J. Lipid Res. 38*, 2134−2146.
89. Smithrud, D. B., Wyman, T. B., and Diederich, F. (1991) *J. Am. Chem. Soc. 113*, 5420−5426.
90. Izatt, R. M., Bradshaw, J. S., Pawlak, K., Bruening, R. L., and Tarbet, B. J. (1992) *Chem. Rev. 92*, 1261−1354.
91. Rekharsky, M. V., and Inoue, Y. (1998) *Chem. Rev. 98*, 1875−1917.
92. Gray, D. M. (1996) in *Circular Dichroism and the Conformational Analysis of Biomolecules* (Fasman, G. D., Ed.) pp 469−500, Plenum Press, New York.
93. Edmundson, A. B., Guddat, L. W., Shan, L., Fan, Z.-C., and Hanson, B. L. (1994) in *55th Forum in Immunology* (Bentley, G. A., Ed.) Institute Pasteur/Elsevier, Paris.
94. Braden, B. C., Goldman, E. R., Mariuzza, R. A., and Poljak, R. J. (1998) *Immunol. Rev. 163*, 45−57.
95. Rubin, C. M., and Schmid, C. W. (1980) *Nucleic Acids Res. 8*, 4613−4619.
96. McCarthy, J. G. (1989) *Nucleic Acids Res. 17*, 7541.
97. Ross, S. A., and Burrows, C. J. (1996) *Nucleic Acids Res. 24*, 5062−5063.
98. Lilley, D. M. J. (1995) *Proc. Natl. Acad. Sci. U.S.A. 92*, 7140−7142.
99. Woodson, S. A., and Crothers, D. M. (1988) *Biochemistry 27*, 3130−3141.
100. Morden, K. M., Chu, Y. G., Martin, F. H., and Tinoco, I. J. (1983) *Biochemistry 22*, 5557−5563.
101. Lum, K., Chandler, D., and Weeks, J. D. (1999) *J. Phys. Chem. B 103*, 4570−4577.
102. Besseling, N. A. M., and Lyklema, J. (1997) *J. Phys. Chem. B 101*, 7604−7611.
103. Cheng, Y.-K., and Rossky, P. J. (1998) *Nature 392*, 696−699.
104. Cheng, Y.-K., and Rossky, P. J. (1999) *Biopolymers 50*, 742−750.
105. Dickinson, R., Franks, N. P., and Lieb, W. R. (1993) *Biophys. J. 64*, 1264−1271.
106. Faergeman, N. J., Sigurskjold, B. W., Kragelund, B. B., Andersen, K. V., and Knudsen, J. (1996) *Biochemistry 35*, 14118−14126.
107. Yoshida, T., Tanaka, M., Mori, Y., and Ueda, I. (1997) *Biochim. Biophys. Acta 1334*, 117−122.
108. Seelig, J., and Ganz, P. (1991) *Biochemistry 30*, 9354−9359.
109. Wenk, M. R., and Seelig, J. (1997) *Biophys. J. 73*, 2565−2574.
110. Smithrud, D. B., and Diederich, F. (1990) *J. Am. Chem. Soc. 112*, 339−343.
111. Carey, J., and Uhlenbeck, O. C. (1983) *Biochemistry 22*, 2610−2615.
112. Hall, K. B., and Kranz, J. K. (1995) *Methods Enzymol. 259*, 261−281.
113. Mossing, M. C., and Record, M. T. J. (1985) *J. Mol. Biol. 186*, 295−305.
114. Draper, D. E. (1993) *Proc. Natl. Acad. Sci. U.S.A. 90*, 7429−7430.
115. Grunwald, E., and Steel, C. (1995) *J. Am. Chem. Soc. 117*, 5687−5692.
116. Liu, L., Yang, C., and Guo, Q.-X. (2000) *Biophys. Chem. 84*, 239−251.
117. Lumry, R., and Rajender, S. (1970) *Biopolymers 9*, 1125−1227.
118. Inoue, Y., Liu, L., Tong, L.-H., Shen, B.-J., and Jin, D.-S. (1993) *J. Am. Chem. Soc. 115*, 10637−10644.

BI0023854